A Microwave Frequency Reference Based on VCSEL-Driven Dark Line Resonances in Cs Vapor

J. Kitching, S. Knappe, N. Vukičević, L. Hollberg, R. Wynands, and W. Weidmann

Abstract—Dark line resonances, narrowed with a buffer gas to less than 100 Hz width, are observed in a Cs vapor cell using a directly modulated vertical-cavity surface-emitting laser (VCSEL). An external oscillator locked to one of these resonances exhibits a short-term stability of $\sigma_y(\tau) = 9.3 \times 10^{-12}/\sqrt{\tau}$, which drops to 1.6×10^{-12} at 100 s. A physics package for a frequency-reference based on this design could be compact, low-power, and simple to implement.

Index Terms—Atomic clock, frequency reference, VCSEL, vertical-cavity surface-emitting laser.

I. INTRODUCTION

NOT LONG after the discovery of dark line resonances [1] and their explanation as being due to coherent population trapping [2] (CPT), these narrow features were recognized as possible microwave frequency references. Studies of a variety of clock geometries based on Λ-resonances were undertaken using tunable dye lasers, atomic beams [3], [4], [5] and vapor cells [6], [7]. Despite difficulties in controlling AC Stark shifts caused by the optical fields, short-term stabilities in the range of $5 \times 10^{-11}/\sqrt{\tau}$ were obtained. The development of diode lasers tunable to alkali-atom optical transitions created new possibilities for using these resonances in compact frequency references. These lasers have been used for optical pumping in optical-microwave double-resonance experiments [8], [9], [33], in dark-line resonance CPT systems [10]–[13], [14]–[16] and in Raman-scattering-based references [17]. The emerging availability of high-quality single-spatial and -spectral mode VCSEL's [18]–[20], now promises more robust, reliable, lower power, and very compact frequency references and magnetometers [21].

In addition to this new enabling technology, there is a rapidly growing need for improved performance from low-cost, compact frequency references [22]. New demanding applications include modern communication networks and GPS receivers which often require devices with performance specifications which are difficult to achieve with quartz crystals but which still need to be small, of low power, and reliable.

J. Kitching is with JILA, The University of Colorado, Boulder, CO 80302 USA, and also with the Time and Frequency Division, The National Institute of Standards and Technology, Boulder, CO 80303 USA (e-mail: kitching@boulder.nist.gov).

N. Vukičević, and L. Hollberg are with the Time and Frequency Division, The National Institute of Standards and Technology, Boulder, CO 80303 USA.

S. Knappe and R. Wynands are with the Institut für Angewandte Physik, Universität Bonn, D-53115, Bonn, Germany.

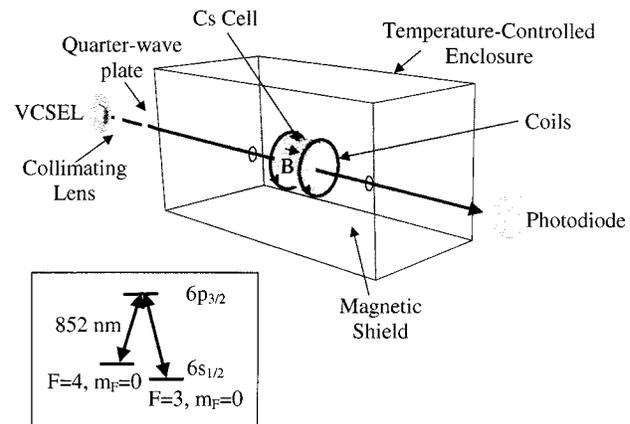W. Weidemann is with Odetics Telecom, Anaheim, CA 92802 USA.

Fig. 1. Physics package used in the experiment. The inset shows the three-level Λ-configuration used to excite the dark-line resonance.

In this work, dark line resonances in Cs vapor are studied for potential use in a compact, low-power, microwave frequency reference. The resonance is excited using light from a VCSEL [21] and detected using the change in dc absorption, resulting in an extremely simple physics package with very high tolerance to misalignment and potentially low acceleration sensitivity. We anticipate engineering the package developed here into a device with a volume less than 1 cm $\times$ 1 cm $\times$ 2 cm and a power dissipation of much less than 100 mW, depending on the thermal environment.

II. A VCSEL-BASED FREQUENCY REFERENCE

The essential components of the optical part of the system are shown in Fig. 1. The VCSEL used to excite the dark line resonance was an oxide-confined structure [19], [20] with a threshold current of 0.82 mA at 31.2 °C and which delivered 870 μW of optical power in a single linear polarization at an operating current of 4.06 mA. The laser linewidth was measured to be $\approx$50 MHz by beating the output with light from a narrow-linewidth ($\Delta\nu \approx$ 2 MHz) distributed-Bragg-reflector (DBR) laser. The VCSEL wavelength was tuned to the Cs D_2 line (852 nm) by carefully controlling the laser temperature and injection current. The light was then collimated and passed through a quarter-wave plate to make the polarization circular before being sent to a cell 2 cm long and containing natural Cs at its vapor pressure along with 8.7 kPa of Ne buffer gas. Buffer gases of this type have long been known to reduce the transit-time and Doppler broadening which occurs in cells containing Cs alone [23]. The cell was placed inside a cylindrical magnetic shield with a transverse field attenuation factor of 2000 to reduce stray magnetic fields. A longitudinal
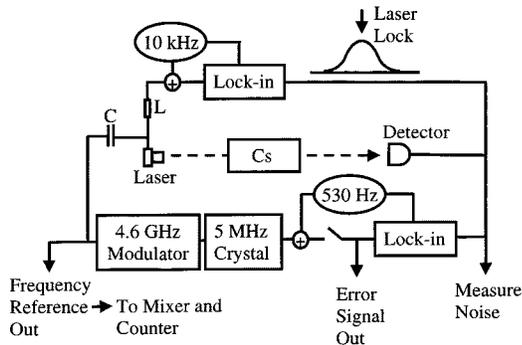
Fig. 2.   Electronics and servo systems used to (a) lock the laser to the absorption profile and (b) lock the crystal oscillator to the dark-line resonance.

Fig. 3.   RF error signal at 4.6 GHz used to lock the external oscillator to the dark line resonance. The resonance width is ≈ 100 Hz and the output low-pass filter time constant was 33 ms. The flat-topped shape is a result of the 530 Hz modulation frequency being roughly equal to the resonance width.

magnetic field of 1×10^{-5} T was applied with a pair of Helmholtz coils to isolate the $m = 0 \rightarrow m = 0$ transition from the other $\Delta m = 0$ transitions. The shield and cell were placed inside a styrofoam enclosure, thermally isolating them from the room, and the cell itself was heated to 29°C and stabilized using active temperature control. The residual temperature fluctuations of a thermistor placed on the cell side wall were on the order of 100 μK. To avoid large light shifts and power broadening of the dark line, the light was intentionally attenuated such that only ≈ 8 μW of optical power in a 4 mm diameter beam was incident on the cell. The power transmitted through the cell was detected with a large-area Si photodiode.

The laser injection current was modulated near 4.6 GHz with 12.6 mW of RF power. A substantial fraction of the optical power was transferred to sidebands on the optical carrier: we estimate that 60% of the original optical power was contained in the first-order sidebands at 4.6 GHz, while only 13% remained in the carrier. A substantial asymmetry in the sideband power was also observed, which we attribute to the effects of correlated simultaneous AM and FM modulation on the laser: the blue sideband contained roughly twice as much power as the red sideband. The remainder (27%) of the optical power was observed in higher-order sidebands. The laser was tuned such that the carrier was half way between the two hyperfine ground-state transitions. The first-order sidebands were therefore resonant with optical transitions from the two ground-state hyperfine levels to the $6P_{3/2}$ excited state forming the three-level Λ-system required for CPT (see inset, Fig. 1).

As the laser sideband frequencies were scanned together over the two Cs resonances, a roughly Lorentzian absorption profile was observed in the transmitted optical power with a full width of 1.4 GHz and a peak absorption of 26%. This Lorentzian profile is a result of the large homogeneous broadening induced by collisions of the Cs atoms with the buffer gas. The laser frequency was locked to the peak of this absorption profile by modulating the laser current at 10 kHz and using lock-in detection as shown in Fig. 2. The resulting laser frequency excursion was roughly 10 MHz. The detuning from the exact line center could be varied by using a voltage offset at the integrator input.

The 4.6 GHz RF modulation applied to the laser was synthesized from a 5 MHz precision crystal oscillator. When the RF modulation frequency was exactly equal to one half the hyperfine splitting of the Cs $6S_{1/2}$ ground state, the sideband ab-
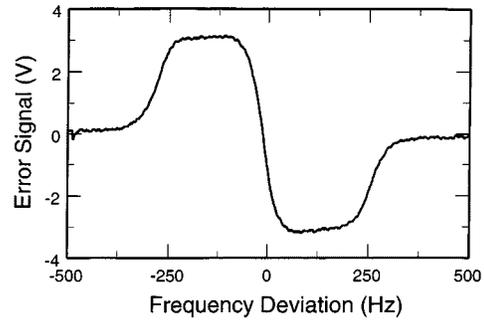
sorption peak height was reduced by $\approx 0.5\%$ due to the CPT effect. At 8 μW of optical power in a 4 mm diameter beam, the resonance width was observed to be ≈ 100 Hz FWHM (out of 4.6 GHz). The crystal frequency itself was modulated at 530 Hz with an amplitude such that the phase modulation index of the 4.6 GHz modulation was 0.6 (see Fig. 2). Lock-in detection was used to produce an error signal to feed back into the crystal. A typical error signal, observed with an output low-pass-filter time constant of 33 ms, is shown in Fig. 3. The flat-topped shape results from the large modulation index and the fact that the modulation frequency was of the same order as the resonance width.

The external oscillator used to modulate the VCSEL was then locked to the narrow resonance, creating a stable frequency reference. A unity-gain frequency substantially higher than one Hertz was used to servo the crystal. The synthesizer output frequency was therefore a faithful representation of that resulting from the atomic signal for integration times longer than one second despite the crystal's short-term stability being somewhat better than that resulting from the atomic signal (as is usually the case with atomic frequency references). The synthesizer signal was then mixed down to 3.36 MHz by beating it against a 9.2 GHz dielectric resonator oscillator, phase-locked to a hydrogen maser and divided to 4.6 GHz with a low-noise digital prescaler. The 3.36 MHz signal was then sent to a counter that used the hydrogen maser signal as a reference. The noise floor of the measurement system with a one-second gate time was $5 \times 10^{-13}/\sqrt{\tau}$, where τ is the integration time, bottoming out near 10^{-14}.

III. FREQUENCY REFERENCE STABILITY AND NOISE

A typical Allan deviation for the frequency reference is shown in Fig. 4. The short-term stability is $9.3 \times 10^{-12}/\sqrt{\tau}$ and is determined by the formula [24]

$$\sigma_y(\tau) = \frac{1}{f_0} \sqrt{\frac{\Delta f_{sig}^2}{\Delta V_{sig}^2} \frac{S_{\Delta V}}{2}} \frac{1}{\sqrt{\tau}}. \qquad (1)$$

Here, f_0 is the RF frequency, $\Delta V_{sig}/\Delta f_{sig}$ is the slope of the error signal at the lock point, $S_{\Delta V}$ is the low-frequency voltage noise power spectral density at the lock-in output and τ is the integration time. It is clear from (1) that the oscillator's stability depends on the slope of the CPT resonance error signal and the low-fre-
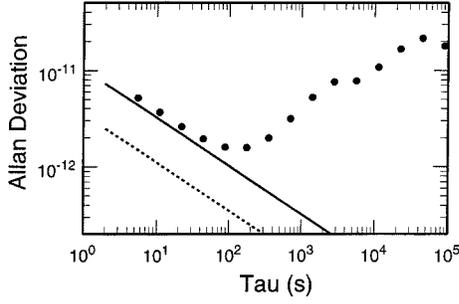
Fig. 4. Allan deviation of the frequency reference. The points show the experimental data while the solid line is calculated from measurements of the open-loop signal-to-noise ratio and the dashed line is the calculated limit due to the AM noise of the laser.
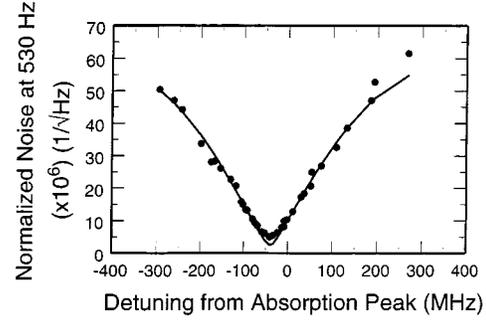

Fig. 5. Detector voltage noise at 530 Hz, normalized to the absorption peak height, as a function of the detuning of the laser frequency from the dc absorption peak center. The solid line is the calculated noise based on the noise processes discussed in the text with an offset of 40 MHz.

quency noise on this signal. The height and width of the CPT resonance have been studied previously as a function of various experimental parameters (laser power and detuning, buffer gas pressure, etc.) [21], [25], [26]; we believe our system is roughly optimized from this point of view. We therefore focus mainly on understanding and reducing the noise, which is determined almost entirely by laser power and frequency fluctuations.

The low-frequency noise on the error signal is determined by the detector's output-voltage noise at 530 Hz. We consider three origins of this noise: power fluctuations of the laser, linear FM–AM conversion on the side of the absorption line, and nonlinear FM–AM conversion near the line peak. With the large optical attenuation used in this experiment, the laser power fluctuations are close to the shot-noise limit and contribute a fractional frequency instability about one third of that measured in the experiment. The limit to the Allan deviation from this noise source at the stated power level is shown by the dashed line in Fig. 4.

In general, laser FM–AM noise conversion in an optically thick resonant medium is a complicated nonlinear process involving the mutual interaction of the laser frequency noise with the fluctuating atomic susceptibility [27]–[30]. However, the optical thickness of our vapor cell is not particularly large, and the laser linewidth is quite small compared to the buffer gas-broadened optical transition width. We therefore approximate this process by assuming simply that the FM noise is converted into AM noise in a linear fashion by the slope of the absorption profile. If the detector voltage as a function of laser detuning, f, is given by

$$V_{\text{det}}(f) = \frac{V_0 \Delta^2}{f^2 + \Delta^2} \qquad (2)$$

then fluctuations in detector voltage are related to fluctuations in laser frequency by

$$\delta V_{\text{det}}(t) = \frac{dV}{df} \, \delta f(t). \qquad (3)$$

This approximation neglects the effects of the FM noise on the real part of the atomic susceptibility and the resulting higher-order contributions that the modified refractive index makes to the AM (and FM) noise on the transmitted field.

While this linear FM–AM noise component is considerable, it should vanish at zero detuning since the slope at this point

is zero. In this case, second-order mixing of FM noise at two different frequencies due to the quadratic transfer function can become the dominant FM–AM noise source. In this case,

$$\delta V_{\text{det}}(t) = \frac{d^2V}{df^2} \, \delta f^2(t) \approx \frac{-2V_0}{\Delta^2} \, \delta f^2(t) \qquad (4)$$

if $V(f)$ is determined by (2). We have identified three possible mixing processes that appear to contribute to the noise when the laser is tuned to the center of the sideband absorption spectrum. The first is the mixing of the laser frequency modulation at 10 kHz (used to lock the laser to the line center) with noise at 10 kHz $\pm$ 530 Hz. Measurements of this effect indicate a contribution to the Allan deviation of about one half the measured value. The second is the mixing of signals at multiples of 60 Hz, which exist due to pickup from the power line, with noise 530 Hz away; this contributes to the Allan deviation at a level about one fifth the measured value. The final mixing process is low-frequency FM noise of the laser with laser FM noise near 530 Hz. An equivalent viewpoint is that low-frequency FM noise of the laser generates a finite rms laser detuning from the resonance peak, resulting in a nonzero linear FM–AM conversion of noise near 530 Hz. Numerical estimates indicate that this contribution to the Allan deviation is about one-tenth of the experimentally measured value.

A plot of the detector noise at 530 Hz, normalized to the absorption peak height, as a function of laser detuning from the absorption-peak maximum is shown in Fig. 5. As expected, the noise shows a minimum near the line center. The solid line in the figure is the calculated noise spectrum based on the processes outlined above, with the linear FM–AM conversion noise dominating far from the absorption peak maximum and the other processes contributing near the noise minimum. The model adequately predicts both the magnitude and shape of the noise as a function of detuning. The Allan deviation calculated from the minimum noise corresponds closely to the measured value at short times (indicated by the solid line in Fig. 4).

There are two noteworthy features of the data in Fig. 5. The first is that the noise minimum occurs away from the absorption line center. Secondly, the quadratic sum of the noise due to the processes outlined above does not altogether account for the minimum noise obtained in the experiment; the experimental noise level remains about 50% larger than the calculated value. We believe that the shifted noise minimum is a result of optical

pumping in combination with the atomic excited-state hyperfine structure [31]. Briefly, the dc absorption is determined by two factors: the populations of the two ground-state hyperfine levels, and the shape of the single-photon absorption profile from each of these levels. Since each of the ground-state hyperfine levels couples to a different set of excited-state hyperfine levels (due to selection rules), the two absorption profiles are frequency shifted with respect to one another by an amount comparable to the excited-state hyperfine splitting.

As the laser is scanned slowly over the line, the ground-state level populations change because of optical pumping, resulting in a distortion of the dc absorption lineshape. However, for laser FM modulation that is faster than the optical pumping time, the level populations remain constant and the resulting change in the absorption is determined exclusively by the single-photon absorption profiles. As a result, the peak of the dc absorption profile (which includes optical pumping) can differ slightly from the minimum of the linear FM–AM conversion (which, for fast modulation, does not depend on the optical pumping). We estimate the optical pumping time to be 1 ms for the power levels used in the experiment; the minimum noise at 500 Hz will therefore be shifted from the peak of the dc absorption by an amount related to the excited-state hyperfine splitting, consistent with the observed shift of 40 MHz.

It may be that the excess noise measured experimentally but still unaccounted for in the model is a result of the nonlinear FM–AM conversion [28], [30] neglected in our model. The conditions that exist in the experiment (small optical thickness, laser linewidth $\ll$ homogeneous linewidth) should minimize this process, but there may be some residual noise of this type still present. While it may be possible that there is some fundamental source of noise we have not accounted for, we anticipate being able to reduce the Allan deviation even further with a more careful choice of operating parameters such as the frequency and index of the modulation used to derive the RF error signal.

At longer times, the Allan deviation appears to be dominated by thermal drifts; the measured change of frequency with time correlates well with changes in ambient temperature. The change in fractional output frequency with cell temperature was measured to be 10^{-9}/K with this buffer gas composition and pressure. A cell temperature stability of 100 μK would therefore translate into a long-term instability of 10^{-13}, far below the measured value. We believe that the residual frequency instability at long times is caused by temperature fluctuations of the cell windows, which are not as well controlled as those of the cell walls due to the need for optical access. Other causes such as changes in laser power or RF coupling into the laser with temperature are also possible, however. Also, combinations of buffer gases are well known to reduce the temperature dependence of the hyperfine frequency shift for cell standards.

IV. UTILITY AS A MICROWAVE FREQUENCY REFERENCE

This work is closely related to that of Cyr et al., [12] and Vanier et al. [13]–[16], who have also used a directly modulated diode laser to excite a coherence between the hyperfine ground states of alkali atoms in vapor cells. Rather than measuring the field absorption, they instead monitor the polarization change of a probe beam [12] or the atomic fluorescence and coherent microwave emission [13]–[16], as the modulation frequency is scanned over the hyperfine splitting. Operating the system as a frequency standard, Vanier et al. [13]–[16] obtain similar stabilities to those reported here. However, the VCSEL used in the present experiment has definite advantages over the extended-cavity laser used in [13]–[16] from the point of view of compactness, power dissipation, and cost. The much larger laser linewidth characteristic of VCSEL's does cause additional FM–AM conversion noise over what might be expected for a narrow-linewidth laser, but the performance is still within a factor of two of the AM noise limit at the optimum laser detuning. We conclude that the use of a VCSEL only marginally degrades the stability of the resulting frequency reference.

The stabilities reported here are by no means competitive with other state-of-the-art frequency references [32]. However, while the ultimate size and power requirements will depend largely on the operational environment and the scale of integration for the electronics, it appears that the physics package described here could be engineered into an extremely small, inexpensive physics package with low power consumption. The opto-electronic components (VCSEL and detector) are manufactured as low-cost commercial products, no optical isolator is used, and the only required optics are a single collimating lens, a quarter-wave plate and a neutral-density filter. Neglecting for now the considerations of cell lifetime and wall losses, the cell diameter is limited only by the laser-beam size of 4 mm. In addition, the laser operates on less than 10 mW of electrical power, and only 12 mW of RF power is required for the modulation. The only other significant power requirement is that needed to control the temperature of the cell and the laser. Finally, the most sensitive alignment issue is that the laser beam must go through the exact center of the Helmholtz coils. We anticipate a low acceleration sensitivity because of this. One disadvantage of this system is that it requires an external oscillator, such as a synthesized crystal or VCO, to lock to the resonance. Issues related to locking an external oscillator to the narrow resonance will need to be addressed before the physics package presented here could be incorporated into a real device.

An important systematic effect in all optically pumped frequency references is the AC Stark shift due to the presence of the optical field. This shift can, for example, cause the output frequency to drift if the intensity of the light changes over time. For an ideal Λ-resonance (with no ground state decoherence), the dark state absorbs no photons from the optical fields and the Stark shift should therefore be identically zero. However, because of the excited state hyperfine structure, Stark shifts result from two sources. First, the $F = 2$ and $F = 5$ excited hyperfine levels do not form Λ-systems with the ground states because of selection rules. The dark state is therefore coupled to these levels via single-photon transitions and associated Stark shifts are present. Secondly, the $F = 3$ and $F = 4$ excited states form two *simultaneous* Λ-systems with the $F = 3$ and $F = 4$ ground states. Since the dark state for one Λ-system may not be dark for the other, single-photon absorption can again occur resulting in a nonzero Stark shift.

The magnitude of this shift is determined by the optical intensity and the detuning from resonance, as well as the buffer-gas pressure. For the buffer gas pressures used in the experiment, the shift is typically of order 0.2 Hz/(μW/cm^2). Because two optical fields are present, the individual shifts from each field can cancel to some extent at certain detunings and optical power ratios leading to a reduced net shift. But the complex structure of excited hyperfine states makes if difficult to predict quantitatively how this occurs.

V. CONCLUSIONS

We have presented a potentially compact, low-power frequency reference with a demonstrated fractional-frequency instability of $< 3 \times 10^{-11}$ between 1 s and 10^5 s of integration time. The short-term stability is limited by a combination of VCSEL AM noise and FM–AM conversion on the atomic resonance. We believe the long-term stability to be limited by residual temperature fluctuations of the Cs vapor cell. The performance level achieved with this very simple system may already meet the performance requirements of communication systems [22] and instrumentation, and numerous improvements in both the basic design and device engineering appear possible.

ACKNOWLEDGMENT

REFERENCES

[1] G. Alzetta, A. Gozzini, L. Moi, and G. Orriols, "An experimental method for the observation of the RF transitions and laser beat resonances in oriented Na vapor," *Nuovo Cimento*, vol. B 36, pp. 5–20, 1976.

[2] E. Arimondo and G. Orriols, "Nonabsorbing atomic coherences by coherent two-photon transitions in a three-level optical pumping," *Lett. Nuovo Cim.*, vol. 17, pp. 333–338, 1976.

[3] J. E. Thomas, S. Ezekiel, C. C. Leiby Jr., R. H. Picard, and C. R. Willis, "Ultrahigh-resolution spectroscopy and frequency standards in the microwave and far-infrared regions using optical lasers," *Opt. Lett.*, vol. 6, pp. 298–300, 1981.

[4] J. E. Thomas, P. R. Hemmer, S. Ezekiel, C. C. Leiby, Jr., R. H. Picard, and C. R. Willis, "Observation of Ramsey fringes using a stimulated, resonance Raman transition in a sodium atomic beam," *Phys. Rev. Lett.*, vol. 48, pp. 867–870, 1982.

[5] P. R. Hemmer, S. Ezekiel, and C. C. Leiby Jr., "Stabilzation of a microwave oscillator using resonance Raman transition in a sodium beam," *Opt. Lett.*, vol. 8, pp. 440–442, 1983.

[6] M. Poelker, P. Kumar, and S.-T. Ho, "Laser frequency translation: A new method," *Opt. Lett.*, vol. 16, pp. 1853–1855, 1991.

[7] P. Kumar and J. H. Shapiro, "Observation of Raman-shifted oscillation near the sodium D lines," *Opt. Lett.*, vol. 10, pp. 226–228, 1985.

[8] C. Rahman and H. G. Robinson, "Rb 0-0 hyperfine transition in evacuated wall-coated cell at melting temperature," *IEEE J. Quantum Electron.*, vol. QE-23, pp. 452–454, 1987.

[9] M. Hashimoto and M. Ohtsu, "Experiments on a semiconductor laser pumped Rubidium atomic clock," *IEEE J. Quantum Electron.*, vol. QE-23, pp. 446–451, 1987.

[10] A. M. Akulshin, A. A. Celikov, and V. L. Velichansky, "Subnatural absorption resonances on the D1 line of Rubidium induced by coherent population trapping," *Opt. Commun.*, vol. 84, pp. 139–143, 1991.

[11] P. R. Hemmer *et al.*, "Semiconductor laser excitation of Ramsey fringes by using a Raman transition in a cesium atomic beam," *J. Opt. Soc. Amer. B, Opt. Phys.*, vol. 10, pp. 1326–1329, 1993.

[12] N. Cyr, M. Tetu, and M. Breton, "All-optical microwave frequency standard: A proposal," *IEEE Trans. Instrum. Meas.*, vol. 42, pp. 640–649, 1993.

[13] J. Vanier, A. Godone, and F. Levi, "Coherent population trapping in cesium: Dark lines and coherent microwave emission," *Phys. Rev. A*, vol. 58, pp. 2345–2358, 1998.

[14] A. Godone, F. Levi, and J. Vanier, "Coherent microwave emission in cesium under coherent population trapping," *Phys. Rev. A*, vol. 59, pp. R12–R15, 1999.

[15] F. Levi, A. Godone, and J. Vanier, "Cesium microwave emission without population inversion," *IEEE Trans. Ultrason., Ferroelect., Freq. Contr.*, vol. 46, pp. 609–615, 1999.

[16] A. Godone, F. Levi, and J. Vanier, "Coherent microwave emission without population inversion: a new atomic frequency standard," *IEEE Trans. Instrum. Meas.*, vol. 48, pp. 504–507, 1999.

[17] N. Vukicevic, A. S. Zibrov, L. Hollberg, F. L. Walls, J. Kitching, and H. G. Robinson, "Compact diode-laser based rubidium frequency reference," *IEEE Trans. Ultrason., Ferroelect., Freq. Contr.*, 2000.

[18] K. Iga, F. Koyama, and S. Kinoshita, "Surface-emitting semiconductor lasers," *IEEE J. Quantum Electron.*, vol. 24, pp. 1845–1855, 1988.

[19] M. Grabherr *et al.*, "Efficient single-mode oxide-confined GaAs VCSEL's emitting in the 850-nm wavelength regime," *IEEE Photon. Technol. Lett.*, vol. 9, pp. 1304–1306, 1997.

[20] J. K. Guenter, R. A. Hawthorne, D. N. Granville, M. K. Hibbs-Brenner, and R. A. Morgan, "Reliability of proton-implanted VCSEL's for data communications," in *Proc. SPIE*, vol. 2683, 1996, pp. 102–112.

[21] C. Affolderbach *et al.*, Nonlinear spectroscopy with a vertical-cavity surface-emitting laser. *Appl. Phys. B* [Online]published online 30 Nov. 99 under DOI 10.1007/s003 409 900 133

[22] J. A. Kusters and C. A. Adams, *RF Design*, May 1999, pp. 28–38.

[23] W. Happer, "Optical pumping," *Rev. Mod. Phys.*, vol. 44, pp. 169–242, 1972.

[24] J. Vanier and C. Audoin, *The Quantum Physics of Atomic Frequency Standards*. New York: Adam Hilger, 1989.

[25] S. Brandt, A. Nagel, R. Wynands, and D. Meschede, "Buffer-gas-induced linewidth reduction of coherent dark resonances to below 50 Hz," *Phys. Rev. A*, vol. 56, pp. R1063–R1066, 1997.

[26] R. Wynands and A. Nagel, "Precision spectroscopy with coherent dark states," *Appl. Phys. B*, vol. 68, pp. 1–25, 1999.

[27] T. Yabuzaki, T. Mitsui, and U. Tanaka, "New type of high-resolution spectroscopy with a diode laser," *Phys. Rev. Lett.*, vol. 67, pp. 2453–2456, 1991.

[28] J. C. Camparo, "Conversion of laser phase noise to amplitude noise in an optically thick vapor," *J. Opt. Soc. Amer. B, Opt. Phys.*, vol. 15, pp. 1177–1186, 1998.

[29] R. Walser and P. Zoller, "Laser-noise-induced polarization fluctuations as a spectroscopic tool," *Phys. Rev. A*, vol. 49, pp. 5067–5077, 1994.

[30] J. C. Camparo and J. G. Coffer, "Conversion of laser phase noise to amplitude noise in a resonant atomic vapor: The role of laser linewidth," *Phys. Rev. A*, vol. 59, pp. 728–735, 1999.

[31] "The details of this optical pumping effect, including a theoretical model, will be discussed in an upcoming publication.,".

[32] G. Mileti, J. Deng, F. L. Walls, D. A. Jennings, and R. E. Drullinger, "Laser-pumped rubidium frequency standards: new analysis and progress," *IEEE J. Quantum Electron.*, vol. 34, pp. 233–237, 1998.

[33] M. Hashimoto and M. Ohtsu, "A novel method to compensate for the effect of light shift in a rubidium atomic clock pumped by a semiconductor laser," *IEEE Trans. Instrum. Meas.*, vol. 39, pp. 458–462, 1990.

J. Kitching, photograph and biography not available at time of publication.

S. Knappe, photograph and biography not available at time of publication.

N. Vukičević, photograph and biography not available at time of publication.

L. Holleberg, photograph and biography not available at time of publication.

R. Wynands, photograph and biography not available at time of publication.

W. Weidemann, photograph and biography not available at time of publication.